Journal of Nuclear Materials 378 (2008) 167–171

Contents lists available at ScienceDirect

Journal of Nuclear Materials

journal homepage: www.elsevier.com/locate/jnucmat

The high-temperature behaviour of $PuPO_4$ monazite and some other related compounds

Regis Jardin [a], Claudiu C. Pavel [a,b], Philippe E. Raison [a], Daniel Bouëxière [a], Hernan Santa-Cruz [a], Rudy J.M. Konings [a], Karin Popa [b,*]

[a] European Commission, Joint Research Centre, Institute for Transuranium Elements, P.O. Box 2340, 76125 Karlsruhe, Germany
[b] 'Al.I. Cuza' University, Department of Chemistry, 11 – Carol I Boulevard, 700506 Iaşi, Romania

ARTICLE INFO

Article history:
Received 8 February 2008
Accepted 31 May 2008

ABSTRACT

Thermal behaviour and lattice parameters of monazites MPO_4 (M^{3+} = Ce^{3+}, Nd^{3+} and Pu^{3+}) and cheralite $CaTh(PO_4)_2$ were studied using high-temperature X-ray diffraction. Heat treatment under inert atmosphere caused the decomposition of $PuPO_4$ and $CaTh(PO_4)_2$ into the corresponding oxides above 1473 K. The influence of the cation type within the crystallographic structure on the thermal expansion coefficient and the possible cation substitutions are discussed in the frame of nuclear waste management.

1. Introduction

The safe disposal of radioactive elements is a major concern of nuclear industry, the main issue being the potential risk associated with the radiotoxic inventory of long-lived elements such as plutonium and minor actinides (MA) of high-level waste. The misuse of such materials must be prevented to reduce risks proliferation, and the environmental impact resulting from release of these elements into the geosphere. For future fuel cycles, the recycling of plutonium and the minor actinides in GEN-IV reactors is aimed at reducing this potential long-term hazard and at decreasing the overall transuranium elements inventory. However, for plutonium and minor actinides that cannot be re-used in reactors [1,2], immobilization with high-level waste is under consideration [3–5].

On the basis of a number of favourable factors (high actinide content, sintering capability, resistance to aqueous alteration and to radiation damage, etc.), the minerals monazite, cheralite and their solid solutions have been suggested as potential waste form for plutonium and MA [6,7]. The mineral monazite, $LnPO_4$ (Ln = La to Gd, $P2_1/n$ space group), has a remarkable ability to retain significant amounts of Th^{4+} and U^{4+} over geological time scale [6,8]. In the natural systems, the charge-balance for the $Ln^{3+} \leftrightarrow Th^{4+}$ substitution can be achieved by two major reactions [9,10]. In the first, huttonite ($ThSiO_4$) mechanism, incorporation of Th^{4+} occurs in large and small cation sites simultaneously as:

$$Ln^{3+} + PO_4^{3-} \leftrightarrow Th^{4+} + SiO_4^{4-} \quad (1)$$

In the cheralite substitution:

$$2Ln^{3+} \leftrightarrow Th^{4+} + Ca^{2+} \quad (2)$$

exchange takes place only over the large cation position. The product of complete substitution (2) is the mineral $CaTh(PO_4)_2$ known as cheralite (previously often called in the literature brabantite) [11–13].

The Pu^{3+} incorporation in such compounds is possible as the end-member $PuPO_4$ crystallizes in the same monoclinic $P2_1/n$ space group. The first synthesis of $PuPO_4$ was reported by Bjorklund [14] and the compound was further characterised in references [15–17]. Its stability domain under vacuum was established to be between 1273 K (below this limit the compound exists in equilibrium with PuP_2O_7) and 1673 K, temperature at which it starts to decompose in air to PuO_2 [14]. Pure solid solutions (La,-Pu)PO_4 with monazite structure were also synthesised for 10 wt% Pu by precipitation [18] or solid state reaction between phosphates end-members [19]. The monazite–cheralite $Ca_{0.18}Th_{0.18}Pu_{0.18}La_{1.46}(PO_4)_2$ solid solution was obtained from oxide precursors at 1773 K [20], but the microstructure reveals the existence of two secondary phases: PuO_2 and one with the composition Pu:P:O = 1:1:1.

The possibility to incorporate of Pu^{4+} in the monazite structure as a function of the ionic radii was studied in order to test the upper limit of tetravalent actinide content. Solid solutions $CaNp_{1-x}Pu_x(PO_4)_2$ with limited solubility of Pu ($x \leqslant 0.3$) were obtained [21,22]. This was explained by instability of Pu^{4+} relative to Pu^{3+} at higher x. Recently, the plutonium mixed-valent compound $Pu^{3+}_{0.8}Pu^{4+}_{0.6}Ca^{2+}_{0.6}(PO_4)_2$ was obtained and characterized [17]. The valence state of plutonium in monazite and cheralite has been studied by using diffuse reflectance spectroscopy [23], and the conclusion is that plutonium is mainly Pu^{3+} in the absence of the charge compensators.

* Corresponding author. Tel.: +40 232 201316; fax: +40 232 201313.
E-mail address: kpopa@uaic.ro (K. Popa).

0022-3115/$ - see front matter © 2008 Elsevier B.V. All rights reserved.
doi:10.1016/j.jnucmat.2008.05.011

Based on those references, we tested the incorporation of plutonium in monazite–cheralite solid solutions by solid state reaction starting from reactive end-members [24], on the basis of the chemical sequence

$$x\mathrm{CaTh(PO_4)_{2(s)}} + (2-2x-y)\mathrm{LnPO_{4(s)}} + y\mathrm{PuPO_{4(s)}} \rightarrow \mathrm{Ca_xTh_xLn_{2-2x-y}Pu_y(PO_4)_{2(s)}} \quad (3)$$

(Ln = La and Ce). Taking into account literature reports on the thermal stability of $LnPO_4$, $CaTh(PO_4)_2$, and $PuPO_4$ under inert atmosphere [14,17,20], the reaction temperature was selected to be 1673 K. Only for a low Pu-loading the final solid solution was pure monazite [19]; in the others we found traces of Pu_2O_3 (and, eventually, ThO_2). Based on those results, we started to re-evaluate the thermal stability of $PuPO_4$ by thermogravimetry and high-temperature XRD.

The thermal stability and the thermal expansion of $PuPO_4$ are presented in this study, compared to two other monazites ($CePO_4$ and $NdPO_4$) and to $CaTh(PO_4)_2$. To our best knowledge, there are no previous data concerning the thermal expansion coefficients of $CaTh(PO_4)_2$ and $PuPO_4$.

2. Experimental

2.1. Synthesis

Reactor grade plutonium(IV) oxide dissolved in nitric acid was used as plutonium source. Pure end-members MPO_4 ($M^{3+} = Ce^{3+}$, Nd^{3+} and Pu^{3+}) monazites as well as $CaTh(PO_4)_2$ were synthesised using high-purity (99.9% or higher, Merck and Sigma–Aldrich) chemicals by the following procedures.

$PuPO_4$ was prepared by sol–gel reaction starting from Pu(IV)-solution, accordingly with the two-step procedure [15,16], in a glove box operated under nitrogen:

$$\mathrm{Pu(NO_3)_{4(aq)}} + 2\mathrm{(NH_4)_2HPO_{4(aq)}} \rightarrow \mathrm{PuP_2O_{7(s)}} + 4\mathrm{NH_4NO_{3(g)}} + \mathrm{H_2O_{(g)}} \quad (873\ \mathrm{K\ for\ 5\ h\ in\ air}) \quad (4)$$

$$4\mathrm{PuP_2O_{7(s)}} + 2\mathrm{H_{2(g)}} \rightarrow 4\mathrm{PuPO_{4(s)}} + \mathrm{P_4O_{10(g)}} + 2\mathrm{H_2O_{(g)}} \quad (1273\ \mathrm{K\ for\ 10\ h\ under\ Ar/H_2}) \quad (5)$$

The $NdPO_4$ sample was prepared from a concentrated aqueous solution (≈5 mol dm^{-3}) of neodymium, obtained by dissolution of $Nd(NO_3)_3 \cdot 6H_2O$ in distilled water. By addition of 85% H_3PO_4 (10% excess), a gel was obtained, filtered (Robu-Glas sintered filter-crucible, porosity 5) and washed 2–3 times with distilled water. The precipitate was heated in an alumina crucible at 1473 K for 10 h (with heating and cooling ramps of 200 K h^{-1}). The final product was sintered at 1873 K for 5 h (with heating and cooling ramps of 300 K h^{-1}). $CePO_4$ was prepared using an identical procedure, although three weeks of precipitate ageing were necessary in order to obtain pure monazite [25].

$CaTh(PO_4)_2$ was synthesized by solid state reaction, mixing in an agate mortar $CaCO_3$, ThO_2 (stoichiometric amounts) and $(NH_4)_2HPO_4$ (10% excess) in a glove box operated under nitrogen. The mixture was then heated in an alumina crucible at 1473 K for 100 h (with heating and cooling ramps of 100 K h^{-1} and 300 K h^{-1}, respectively) under nitrogen atmosphere. $CaTh(PO_4)_2$ forms in accordance with the general chemical reaction

$$\mathrm{CaCO_{3(s)}} + \mathrm{ThO_{2(s)}} + 2\mathrm{(NH_4)_2HPO_{4(s)}} \rightarrow \mathrm{CaTh(PO_4)_{2(s)}} + \mathrm{CO_{2(g)}} + 3\mathrm{H_2O_{(g)}} + 4\mathrm{NH_{3(g)}}. \quad (6)$$

2.2. High temperature X-ray diffraction analysis

Thermal expansion of the monazites MPO_4 (M = Pu, Ce, and Nd) and $CaTh(PO_4)_2$ were investigated by high-temperature X-ray diffraction (HT-XRD) using a Pt heating strip under helium (4.6). Because the used $PuPO_4$ sample was a half a year old, it was annealed at 1273 K several days before HT-XRD experiment to eliminate possible radiation effects.

The X-ray data were collected using a Siemens D8 diffractometer mounted in a Bragg-Brentano configuration, with a curved Ge monochromator (1 1 1), a ceramic Cu X-ray tube (40 kV, 40 mA), a PSD (Position Sensitive Detector) Braun detector covering 6° in 2θ and was equipped with a Anton Paar HTK2000 heating chamber. Scans were collected from 10° to 110° in 2θ using 0.0146° step-intervals with counting steps of 3 s in the 303–1473 K temperature range in helium atmosphere. In the case of $PuPO_4$ and $CaTh(PO_4)_2$ measurement were performed up to 1673 K in order to observe the phase decomposition. Unit cell parameters were refined on powdered samples by a Le Bail-type method using the Fullprof software.

It is important to note that the heating chamber was firstly calibrated using magnesium oxide MgO (Periclase type) as standard. In the 303–1673 K temperature range, we calculated a thermal expansion coefficient (TEC) of $12.37 \times 10^{-6}\ K^{-1}$ which is in good agreement with previous studies [26–29].

2.3. Thermogravimetric analysis

Thermal behaviour from room temperature up to 1793 K of 45.0 mg of $PuPO_4$ powder was investigated by TG-DSC in a 10 ml min^{-1} argon (4.6) flow with a heating rate of 10 K min^{-1} using a Netzsch STA 409 apparatus. The experimental error is less than 1%.

3. Results

The lattice parameters at room temperature of the monoclinic crystal structure of monazites MPO_4 (M = Pu, Ce, and Nd) and $CaTh(PO_4)_2$ are given in Table 1. Our values are comparable with published data [14,30,31].

The structural and thermal properties of the phosphate samples were investigated by in situ high-temperature powder X-ray diffraction technique. Lattice parameters and volume have been measured at temperature intervals of 100 K in the range 303–1473 K from the refinement. The plots of $\Delta l/l_0$ as a function of temperature are shown in Fig. 1–4. The best fit was obtained using a quadratic function.

Figs. 1–3 show some general trends. The largest lattice parameter (b) has the smallest thermal expansion behaviour compared to a and c parameters. This can be explained by more rigid chains comprising MO_9 nine-vertex polyhedra along the b direction. The parameter β is only slightly affected by temperature and remains almost constant over the entire range.

Comparing the different phosphates investigated in this study, it can be noticed that the parameter a of $CaTh(PO_4)_2$ expands more than that of the monazites MPO_4 (M = Pu, Ce, and Nd) (Fig. 1). A similar behaviour was observed for the b lattice parameter, but to a lesser extent (Fig. 2). From all data fits, including the volume (Fig. 4), it can be noticed that the $PuPO_4$ sample shows a significantly smaller thermal expansion compared to the other compounds. This may originate from the different behaviour of the 4f

Table 1
Lattice parameters at room temperature of MPO_4 (M = Pu, Ce, and Nd) and $CaTh(PO_4)_2$

	$PuPO_4$	$CePO_4$	$NdPO_4$	$CaTh(PO_4)_2$
a (Å)	6.7641(2)	6.7989(2)	6.7426(3)	6.7088(1)
b (Å)	6.9841(2)	7.0226(2)	6.9574(2)	6.9166(9)
c (Å)	6.4536(2)	6.4735(2)	6.4097(3)	6.4158(1)
β (°)	103.640(2)	103.4755(2)	103.6624(3)	103.7031(1)

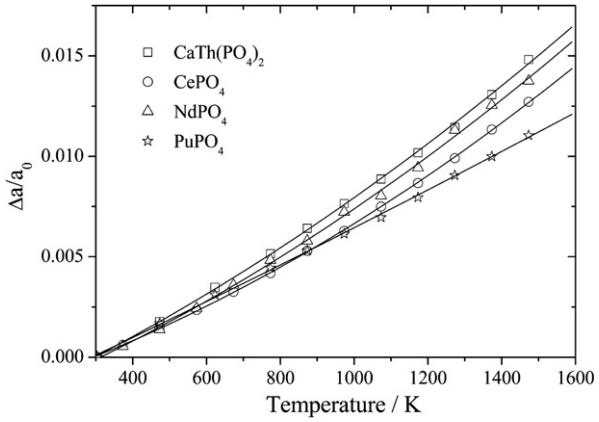

Fig. 1. Thermal expansion along a direction in the temperature range 300–1500 K for $CaTh(PO_4)_2$, $CePO_4$, $NdPO_4$ and $PuPO_4$.

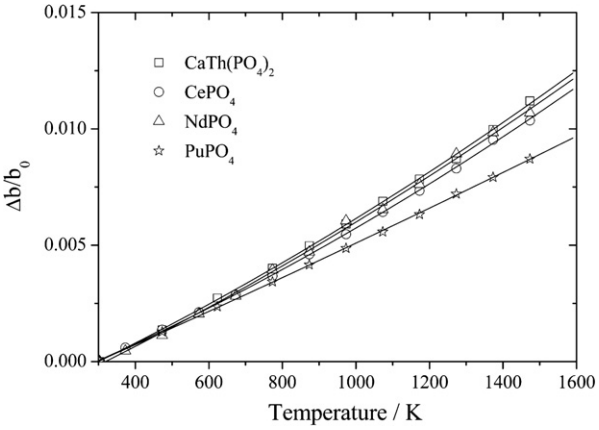

Fig. 2. Thermal expansion along b direction in the temperature range 300–1500 K for $CaTh(PO_4)_2$, $CePO_4$, $NdPO_4$ and $PuPO_4$.

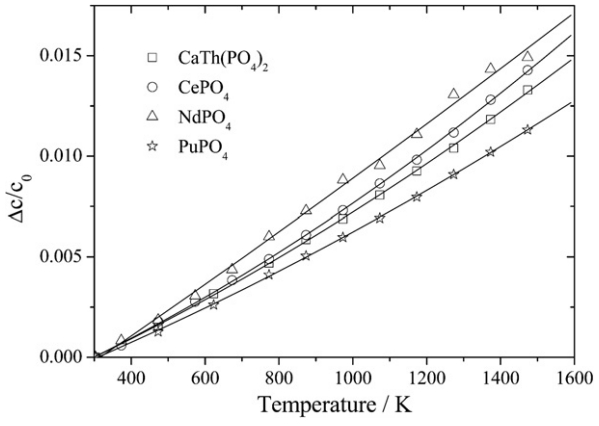

Fig. 3. Thermal expansion along c direction in the temperature range 300–1500 K for $CaTh(PO_4)_2$, $CePO_4$, $NdPO_4$ and $PuPO_4$.

and 5f electrons of the M^{3+} ions in these compounds and from the pivotal position of plutonium in the actinides series [32]. As a result of their itinerant character, the 5f electrons in the early actinides participate in the chemical bonding, unlike the 4f electrons in the lanthanides that are localised.

The mean linear thermal expansion coefficients (α) were obtained by fitting the polynomial equation $\Delta l/l_0 = \alpha \cdot \Delta T + \beta \cdot \Delta T^2$, where l_0 is the lattice parameter at room temperature, over the range from 303 to 1473 K. The lattice thermal expansion coefficients along a (α_a), b (α_b) and c (α_c) directions and the volume thermal expansion coefficients ($\alpha_V = \Delta V/3V$) are given in Table 2. The smallest volume expansion coefficient was observed for $PuPO_4$, followed by $CePO_4$, $CaTh(PO_4)_2$, and $NdPO_4$.

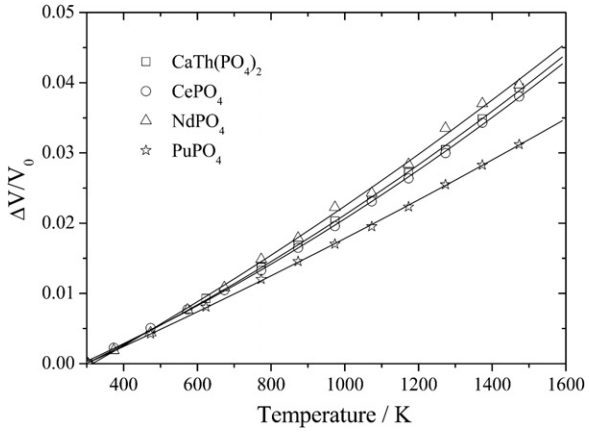

Fig. 4. Thermal expansion in volume in the temperature range 300–1500 K for $CaTh(PO_4)_2$, $CePO_4$, $NdPO_4$ and $PuPO_4$.

The expansion coefficients of $CePO_4$ are not very different from those reported by Bakker et al. [33] calculated from 293 to 1323 K using X-ray diffraction. They found $\alpha_a = 7.32 \times 10^{-6}\,K^{-1}$, $\alpha_b = 7.77 \times 10^{-6}\,K^{-1}$, $\alpha_c = 9.00 \times 10^{-6}\,K^{-1}$ and $\alpha_V = 8.25 \times 10^{-6}\,K^{-1}$, compared to our values, $\alpha_a = 7.48 \times 10^{-6}\,K^{-1}$, $\alpha_b = 7.07 \times 10^{-6}\,K^{-1}$, $\alpha_c = 9.18 \times 10^{-6}\,K^{-1}$ and $\alpha_V = 8.14 \cdot 10^{-6}\,K^{-1}$, calculated up to 1303 K. However, the error of their experimental setup (ca. 10%) was higher than ours (ca. 1–2%). Perrière et al. [34] have extrapolated from dilatometry data that the thermal expansion coefficient for $CePO_4$ is $10.5 \times 10^{-6}\,K^{-1}$, while our value is $8.14 \times 10^{-6}\,K^{-1}$. In case of $NdPO_4$, the same authors reported the value of $10.6 \times 10^{-6}\,K^{-1}$, as obtained from high-temperature XRD over 373−1273 K, compared to $9.26 \times 10^{-6}\,K^{-1}$ (α_V) obtained by us in this work up to 1473 K. The small differences most probable originate from the fact that Perrière et al. [34] have used a linear fit, while we applied a second-order polynomial equation.

$CePO_4$ and $NdPO_4$ were found to be thermally stable throughout temperature interval considered. However, above 1473 K, $CaTh(PO_4)_2$ and $PuPO_4$ start to decompose into the corresponding

Table 2
Thermal expansion coefficients obtained from the expression $\Delta l/l_0 = \alpha\Delta T + \beta T^2$ over range 303–1473 K

		$\alpha\ 10^{-6}$	$\beta\ 10^{-9}$
$PuPO_4$	a (Å)	8.7(3)	3.9(3)
	b (Å)	7.0(1)	0.3(1)
	c (Å)	7.9(2)	1.4(1)
	V (Å^3)	7.9(2)	0.7(1)
$CePO_4$	a (Å)	7.4(1)	2.8(1)
	b (Å)	7.0(2)	1.5(1)
	c (Å)	9.1(2)	2.5(2)
	V (Å^3)	8.1(2)	2.1(2)
$NdPO_4$	a (Å)	8.8(5)	2.6(4)
	b (Å)	7.8(5)	1.2(4)
	c (Å)	12.6(8)	0.5(7)
	V (Å^3)	9.8(6)	1.5(5)
$CaTh(PO_4)_2$	a (Å)	9.6(4)	2.4(3)
	b (Å)	7.7(3)	1.4(2)
	c (Å)	8.9(3)	1.9(2)
	V (Å^3)	8.6(3)	2.0(2)

The standard deviation is comprised between 2% to 6%, higher for $CaTh(PO_4)_2$ and $NdPO_4$ compounds, and smaller for $CePO_4$ and $PuPO_4$ ones.

oxides. For $CaTh(PO_4)_2$ this is in fair agreement with previous reports [35] and with the thermodynamic data for this compound [36], from which we can calculate that the Gibbs energy for the reaction:

$$2CaTh(PO_4)_{2(s)} \rightarrow 2CaO_{(s)} + 2ThO_{2(s)} + P_4O_{10(g)} \quad (7)$$

is zero at $T = 1410$ K. Above this temperature $CaTh(PO_4)_2$ is not stable with respect to the pure oxides.

Fig. 5 shows the XRD patterns of $CaTh(PO_4)_2$ phase at 1473, 1573, and 1673 K. The diffractions at about 27.2 and 31.5° (2θ) correspond to the (111) and the (200) diffractions of ThO_2. The refined unit cell parameter for ThO_2 [5.6008(3) Å at 273 K, 5.6606(3) Å at 1473 K, 5.6691(1) Å at 1573 K and 5.6746(1) Å at 1673 K] are in very good agreement with the data obtained by Tyagi et al. [37], confirming the decomposition mechanisms of $CaTh(PO_4)_2$ in the more stable oxides.

The decomposition of $PuPO_4$ into Pu_2O_3, was observed at 1573 K; the intensity of the specific diffractions of Pu_2O_3 [28.05 and 32.5° (2θ)] increases at higher temperatures (Fig. 6).

The TG-curve (Fig. 7) indicates that $PuPO_4$ starts to decompose at about 1550 K, accordingly with the HT-XRD results, the weight loss being 2.05 wt%. The XRD pattern of the compound collected from the TG device after heating at 1793 K (Fig. 8) indicates the formation of cubic Pu_2O_3 as secondary phase. However, in previous studies [14,20] PuO_2 was found to appear as decomposition product; this is because of the oxidising conditions applied in the mentioned works, which cause Pu-sesquioxide to immediately oxidise

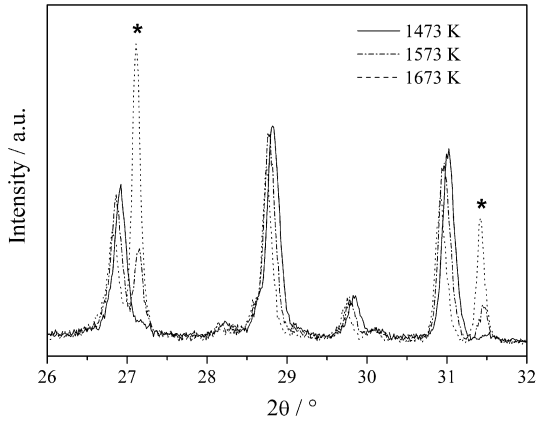

Fig. 5. The X-ray diffraction patterns of the $CaTh(PO_4)_2$ phase at 1473, 1573, and 1673 K. The asterisks correspond to ThO_2 phase.

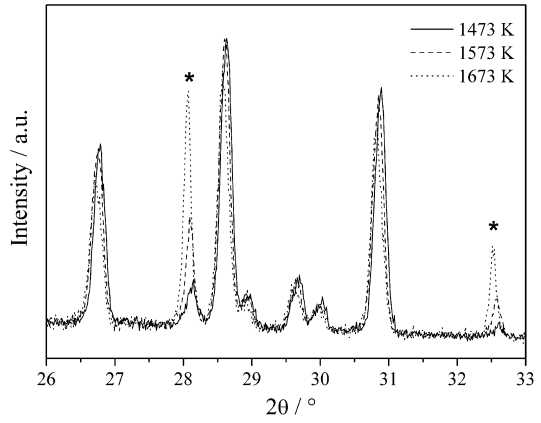

Fig. 6. The X-ray diffraction patterns of the $PuPO_4$ phase at 1473, 1573 and 1673 K. The asterisks correspond to Pu_2O_3 phase.

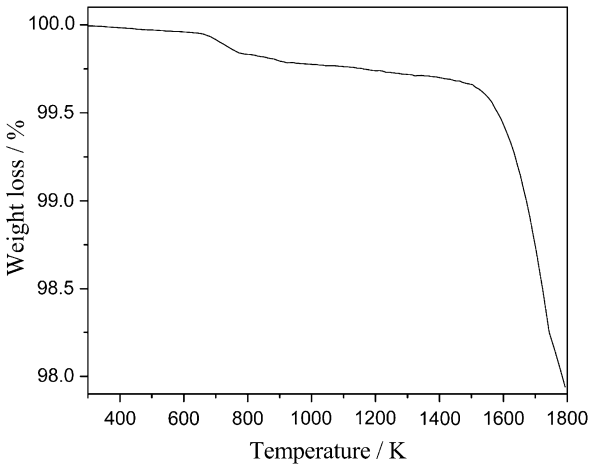

Fig. 7. TG-curve of $PuPO_4$ heated under argon.

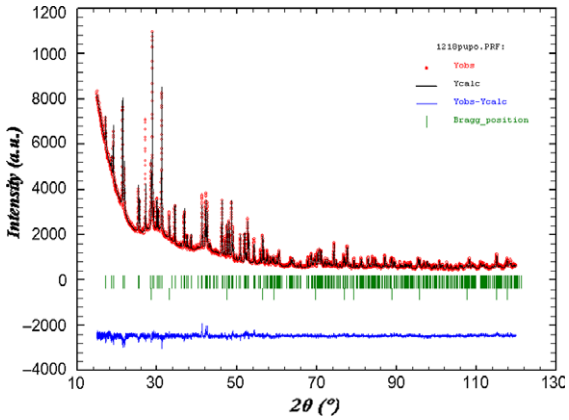

Fig. 8. XRD pattern, fitting and difference curve for $PuPO_4$, used in the thermogravimetric measurement under helium, showing the formation of Pu_2O_3 as secondary phase. The upper Bragg positions correspond to $PuPO_4$, while the lower to Pu_2O_3.

to Pu(IV) dioxide. The chemical reaction which can explain the observed behaviour is

$$4PuPO_{4(s)} \rightarrow 2Pu_2O_{3(s)} + P_4O_{10(g)} \quad (8)$$

The amount of Pu_2O_3 evaluated from the XRD measurement corresponds to 8.2 wt% Pu_2O_3 (3.69 mg). The weight loss associated to the P_4O_{10} release of 2.17 wt% (0.98 mg) is in good agreement with the one observed in the TG experiment. This is in line with the conclusion of Deschanels et al. [20], namely that such compounds are not pure phases at 1523 K.

4. Conclusions

The thermal expansion curves of $PuPO_4$ and some lanthanide counterparts as well as $CaTh(PO_4)_2$ were measured and compared. The dilatation mechanism of the compounds tested is isotropic, even if there are some differences between the three axes. The results indicate that the volume expansion of those phosphate samples are quite similar, except for the $PuPO_4$ case that is systematically lower.

The decomposition of $PuPO_4$ was found to occur at lower temperature than previously reported in the literature [14]. In practice, the decomposition can limit the incorporation of Pu in monazite–cheralite solid solutions since these normally form above 1550 K,

i.e. above the stability limit of $PuPO_4$ in inert atmosphere found here. A similar behaviour was observed in the case of $CaTh(PO_4)_2$. These findings are limiting both for Pu-loading in monazite–cheralite solid solutions via end-members precursors and for the sintering of the Pu-containing monazites. The result of the present study limits the existence domain of the pure Pu-containing compounds with monazite–cheralite structure to the range between 1273 and 1473 K.

Acknowledgements

Authors are grateful to D. Bregiroux and R. Eloirdi for fruitful discussions. CP, HSC, and KP all acknowledge the European Commission for support given in the frame of the program 'Training and Mobility of Researchers'. Participation to the European Commission-JRC-ITU Actinide User Laboratory program (Contract 209657/2007 AUL 101) is also acknowledged.

References

[1] J.M. Haschke, J.L. Stakebake, in: L.R. Morss, N.M. Edelstein, J. Fuger (Eds.), The Chemistry of the Actinide and Transactinide Elements, Springer, 2006, p. 3199.
[2] C. Guy, F. Audubert, J.E. Lartigue, C. Latrille, T. Advocat, C. Fillet, C.R. Physique 3 (2002) 827.
[3] R.C. Ewing, Proc. Natl. Acad. Sci. USA 96 (1999) 3432.
[4] R.C. Ewing, W.J. Weber, J. Lian, J. Appl. Phys. 95 (2004) 5949.
[5] R.C. Ewing, Earth Planet. Sci. Lett. 229 (2005) 165.
[6] G.J. McCarthy, W.B. White, D.E. Pfoertsch, Mater. Res. Bull. 13 (1978) 1239.
[7] L.A. Boatner, B.C. Sales, in: W. Lutze, R.C. Ewing (Eds.), Radioactive Waste Forms for the Future, 1998, p. 495.
[8] A. Meldrum, L.M. Wang, R.C. Ewing, Nucl. Instrum. Meth. Phys. Res. B 116 (1996) 220.
[9] J.M. Montel, J.L. Devidal, D. Avignant, Chem. Geol. 191 (2002) 89.
[10] J.M. Montel, B. Glorieux, A.M. Seydoux-Guillaume, R. Wirth, J. Phys. Chem. Solids 67 (2006) 2489.
[11] Y. Hikichi, K. Hukuo, J. Shiokawa, Nihon-Kagakki-shi (J. Chem. Soc. Jpn.) 12 (1978) 1635.
[12] D. Rose, N. Jb. Miner. Mh. 6 (1980) 247.
[13] J.M. Hughes, E.E. Foord, M.A. Hubbard, Y. Ni, N. Jb. Mineral. Mh. 8 (1995) 344.
[14] C.W. Bjorklund, J. Am. Chem. Soc. 79 (1958) 6347.
[15] C.E. Bamberger, R.G. Haire, H.E. Hellwege, G.M. Begun, J. Less Common Met. 97 (1984) 349.
[16] C. Thiriet, R.J.M. Konings, F. Wastin, J. Nucl. Mater. 344 (2005) 56.
[17] D. Bregiroux, R. Belin, P. Valenza, F. Audubert, D. Bernache-Assollant, J. Nucl. Mater. 366 (2007) 52.
[18] B.E. Burakov, M.A. Yagovkina, V.M. Garbuzov, A.A. Kitsay, V.A. Zirlin, Mater. Res. Symp. Proc. 824 (2004) 219.
[19] K. Popa, E. Colineau, F. Wastin, R.J.M. Konings, Solid State Commun. 144 (2007) 74.
[20] X. Deschanels, V. Picot, B. Glorieux, F. Jorion, S. Peuget, D. Roudil, C. Jégou, V. Broudic, J.N. Cachia, T. Advocat, C. Den Auwer, C. Fillet, J.P. Coutures, C. Hennig, A. Scheinost, J. Nucl. Mater. 352 (2006) 233.
[21] A. Tabuteau, M. Pagès, J. Livet, C. Musikas, J. Less Common Met. 121 (1986) 650.
[22] A. Tabuteau, M. Pagès, J. Livet, C. Musikas, J. Mater. Sci. Lett. 7 (1988) 1315.
[23] Y. Zhang, E.R. Vance, J. Nucl. Mater. 375 (2008) 311.
[24] K. Popa, in: Alternative Materials for Radioactive Waste Stabilization and Nuclear Materials Containment, March 25–29, Barga, Italy, 2007.
[25] K. Popa, D. Sedmidubský, O. Beneš, C. Thiriet, R.J.M. Konings, J. Chem. Thermodyn. 38 (2006) 825.
[26] M. Hazen, Am. Mineral. 61 (1976) 266.
[27] D. Taylor, Trans. J. Brit. Ceram. Soc. 83 (1984) 5.
[28] D.K. Swanson, C.T. Prewitt, J. Appl. Chem. 19 (1986) 1.
[29] R.R. Reeber, K. Goessel, K. Wang, Eur. J. Mineral. 7 (1995) 1039.
[30] Y. Ni, J.M. Hughes, A.N. Mariano, Am. Mineral. 80 (1995) 21.
[31] R. Podor, M. Cuney, Am. Mineral. 82 (1997) 765.
[32] R.G. Haire, J.K. Gibson, in: L.R. Morss, J. Fuger (Eds.), Transuranium Elements. A Half Century, ACS, Washington, DC, 1992, p. 426.
[33] K. Bakker, H. Hein, R.J.M. Konings, R.R. van der Laan, Hj. Matzke, P. van Vlaanderen, J. Nucl. Mater. 252 (1998) 228.
[34] L. Perrière, D. Bregiroux, B. Naitali, F. Audubert, E. Champion, D.S. Smith, D. Bernache-Assollant, J. Euro. Ceram. Soc. 27 (2007) 3207.
[35] D. Bregiroux, O. Terra, F. Audubert, N. Dacheux, V. Serin, R. Podor, D. Bernache-Assollant, Inorg. Chem. 24 (2007) 10372.
[36] K. Popa, T. Shvareva, L. Mazeina, E. Colineau, F. Wastin, R.J.M. Konings, A. Navrotsky, Am. Mineral 93 (2008).
[37] A.K. Tyagi, M.D. Mathews, B.R. Ambekar, R. Ramachandran, Thermochim. Acta 421 (2004) 69.